IEEE Access
Multidisciplinary | Rapid Review | Open Access Journal

Received December 16, 2019, accepted January 5, 2020, date of publication January 13, 2020, date of current version January 31, 2020.

Digital Object Identifier 10.1109/ACCESS.2020.2966430

Optimal Performance of Dynamic Particle Swarm Optimization Based Maximum Power Trackers for Stand-Alone PV System Under Partial Shading Conditions

SERGEY OBUKHOV[1], AHMED IBRAHIM[1,2], AHMED A. ZAKI DIAB[3,4], AMEENA SAAD AL-SUMAITI[5], AND RAEF ABOELSAUD[1,2]

[1]Department of Electrical Engineering, National Research Tomsk Polytechnic University, 6340350 Tomsk, Russia
[2]Department of Electrical Power and Machines Engineering, Zagazig University, Zagazig 44511, Egypt
[3]Department of Electrical and Electronic Engineering, Kyushu University, Fukuoka 819-0395, Japan
[4]Electrical Engineering Department, Faculty of Engineering, Minia University, Minia 61111, Egypt
[5]Advanced Power and Energy Center, Electrical Engineering and Computer Science Department, Khalifa University, Abu Dhabi 127788, UAE

Corresponding authors: Ahmed Ibrahim (ibragim@tpu.ru) and Ahmed A. Zaki Diab (a.diab@mu.edu.eg)

This work was supported in part by Tomsk Polytechnic University within the framework of Tomsk Polytechnic University Competitiveness Enhancement Program, and in part by Khalifa University, Abu Dhabi, United Arab Emirates under Award FSU-2018-25.

ABSTRACT One of the important tasks for increasing the efficiency of photovoltaic (PV) system is the development and improvement of the maximum power point tracking algorithms (MPPT). These MPPT algorithms lead to the ability to catch efficiently the global maximum power point of the partially shaded PV array. One of these trackers is the particle swarm optimization (PSO) algorithm which is one of the Soft computing techniques. The conventional PSO based trackers have many advantages such as the simplicity of hardware implementation and independence from the installed system. The actual problem of the practical application of PSO is the determination of its parameters to ensure high effectiveness of extracting the global MPP. Analysis of scientific papers devoted to the PSO algorithm has shown that there is currently no methodology for the optimal parameters' selection of PSO algorithm based maximum power trackers for the PV system. This paper aims to create a convenient and reasonable method for choosing the optimal parameters of the PSO algorithm, taking into account the topology and parameters of the DC-DC converter and the configuration of solar panels. A new method for selecting the parameters of a buck converter connected to a battery has been presented. The optimal value of the sampling time for the digital MPP controllers, providing their maximum performance; has been determined based on a new methodology. Matlab/Simulink software package is used as the main research tool. The prominent outcomes identify that the modified PSO and its designed parameters best meet the requirements of the MPPT controller for the PV system.

INDEX TERMS MPPT, partial shading, PSO, buck converter, battery, PV.

I. INTRODUCTION

The priority of the development of modern energy is the use of renewable energy sources (RES). There are several merits for RES, for instance, availability, environmental friendliness, and low maintenance. Among the resources of renewable energy, the photovoltaic (PV) modules are one of the most distinguished systems in the world because it has a longer lifespan (Typically more than 20 years), and many several advantages [1]. Solar energy is rapidly developing in many countries of the world, with PV power generation that is showing the greatest dynamics development compared with the other types of RES. According to the latest report of the joint research center (JRC) of the European Commission's science and knowledge service, the installed capacity of PV plants in 2017 reached 408 GW with an average annual increase of more than 40% over the past 15 years [2].

In 2017, solar energy attracted 58% of all new investments in renewable energy of 161 billion US dollars [2]. The major challenge when using PV energy is its strong dependence

The associate editor coordinating the review of this manuscript and approving it for publication was Manoj Datta.

upon the weather conditions. In addition, it is more difficult to extract the maximum power point (MPP) from its nonlinear characteristics (i.e., power-voltage (P-V) characteristics). To solve these problems, numerous of maximum power point tracking (MPPT) techniques have been proposed to catch the optimal operating point of the PV power generation system.

From the point of control, MPPT controllers are divided into two types: analog and digital. In analog controllers, the control signal is generated in the form of a reference voltage, which is compared with the output voltage of the converter, and then the mismatch signal is processed by a traditional control system based on a proportional integral derivative (PID) controller [3]. While in the digital MPPT controllers, the output signal is d (duty cycle), which is fed directly to the converter switch via a pulse width modulation (PWM) generator. Due to the simplicity of implementation and higher reliability of these controllers, they are mainly utilizing in modern PV systems [4]. When using digital controllers, the value of d changes discretely by the value of Δd after a certain sampling time ts, the numerical values of which directly affect the accuracy and tracking speed of the MPP when solar irradiance and temperature of the solar panels are changed.

A variety of conventional techniques such as perturb and observe (P&O) [5], incremental conductance [6], constant voltage [7] and some others [8] have been introduced to extract the MPP of the solar array under uniform solar irradiance of the PV system. Although these approaches show good performance in detecting this maxima, they failed to catch the global maximum power point (GMPP) under partial shading conditions (PSC) of the PV panels. Under PSC of the PV panel, the P-V characteristics get more complex with multiple local peaks (LPs) and one global MPP due to the use of the bypass diodes to withstand the hot spot effect [9].

Recently, several evolutionary optimization techniques have been proposed to mitigate the effect of PSC on the PV arrays. Moreover, they have been utilized to detect the GMPP of the PV panels where the conventional methods fail to converge [9], [10]. For instance, the genetic algorithm (GA) [11], [12], artificial intelligence methods using fuzzy logic and neural networks have been applied to find the GMMP [13], [14]. A detailed review, classification, and comparative analysis of the GMPP algorithms are given in [6], [8]–[10], [15]. The criteria for comparative evaluation of the effectiveness of different GMPP techniques use the simple hardware implementation, cost, speed, and accuracy of tracking GMPP in various operating conditions of the PV panels.

Particle swarm optimization (PSO) has proven itself as the most effective method for determining GMPP of the PV arrays under the PSC. Moreover, it has been considered simple in implementation and faster to extract the optimal solution in many engineering problems [16], [19], [21]. Based on literature studies [18]–[29], the main problem in utilizing the PSO algorithm to detect the GMPP of the PV systems is the selection of its parameters.

Besides, many researchers selected the main parameters of PSO (i.e., number of particles N, the coefficient of the inertia w, acceleration coefficient c_1 and c_2, and the sample time ts) by trial and error without taking into account the topology and the parameters of the DC-DC converter and the configuration of the solar panel [18]–[29].

For instance, in [22], [24]–[26], [28], [29], a proposed PSO algorithm is presented to determine the GMPP of a PV panel based on 3 particles, while 4 particles are utilized for the PSO controller in [16] and [19]. In [17] and [21], 5 particles are used, while reference [23] suggests 6 particles. It is proposed to use 9 particles in [27] whereas 10 particles are utilized in [18].

In [18], [24], [25], [27]–[29], constant values of the acceleration coefficient are proposed. In [23] and [26], a linear decreasing scheme for c_1 and c_2 is suggested, while in [17], [20], [21], a decreasing law for c_1 and a linear increasing law for c_2 are proposed. It is noticed that there are significant differences in the authors' opinion in defining the value of the sample time ts: in [19], [25] and [29], the value of ts was less than 0.01s. Reference [28] was suggested the value of ts for the controller of the PV panel to be 0.06s. In [24] and [26], the ts was selected to be 0.1s, while ts was 0.2s in [17], [21]–[23].

The unreasonable selection of the PSO parameters leads to an increase extracting the GMPP of the PV system and a decrease in the accuracy of MPP efficiency, and as a result leads to a decrease in the overall efficiency of the PV plant. In most of the scientific studies using PSO in its search for GMPP, DC-DC boost converter connected to a resistive load is used [18]–[29]. Accordingly, the obtained research results cannot be utilized in the design of autonomous photovoltaic power plants (Fig.1), in which the construction schemes are mainly based on buck converters connected to a battery charge. The objective of this research is on the design of stand-alone PV system for delivering maximum power to low power consumer that are isolated form the central electrical grid network. Fig. 1 shows a typical scheme of the construction of the autonomous low power PV system. The output voltage and current from the PV panels are fed to the controller unit, which catches the GMPP under PSC and gives the optimal duty cycle to the DC-DC buck converter.

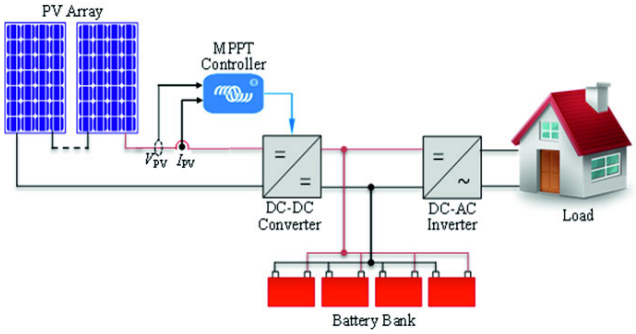

FIGURE 1. Block diagram for the stand-alone PV system.

The main contribution of this paper is to propose a new methodology to select the optimal parameters of the MPP controller of the PV system based on the basic principles of the PSO algorithm. Moreover, this work considers the designing and selecting the parameters of the buck DC-DC power converter, which is connected to the battery by taking into consideration the topology and configuration of the PV panel. Moreover, this paper introduces a new technique for determining the optimal value of the sampling time for the digital MPPT controller, providing their maximum performance.

The remainder of this paper is organized in the following manner. Section II describes the basic mathematical models of the components of the PV system that were used in this research. Section III elaborates on the PSO algorithm and two modified techniques based-PSO that are provided to enhance the performance of the MPP tracker for extracting the GMPP under PSC of the PV system. Section IV deals with the selection and the design of the parameters of autonomous PV system components. Section V discusses the choice of optimal parameters of the PSO controller. The simulation results considering the validation of the proposed algorithm under uniform solar irradiance and fast changes of the solar insolation are presented in section VI. In the conclusion section, the research findings are recapitulated.

II. MATHEMATICAL MODELS OF THE COMPONENTS OF A PHOTOVOLTAIC SYSTEM

A. MODELING OF A PV CELL

A PV array can be represented by the single-diode model shown in Fig. 2 [7]. The mathematical equation that expresses the output current of the PV cell is given as follows [16]:

$$I = I_{PH} - I_D - I_{SH} = I_{PH} - I_0 \cdot \left[\exp\left(\frac{q(V + I \cdot R_S)}{A \cdot k \cdot T}\right) - 1\right] - \frac{V + I \cdot R_S}{R_{SH}} \quad (1)$$

where;

I_{PH} denotes current of the PV array;

A denotes ideality factor (varies from 1 to 2 depends on PV technology);

I_0 denotes reverse saturation current of the diode;

R_S, R_{SH} denote series and parallel resistance, respectively;

T denotes cell temperature in kelvin;

q denotes charge of electron (q= $1.602 \cdot 10^{-19}$ (c));

k denotes Boltzmann constant (k= $1.38 \cdot 10^{-23}$(J/K)).

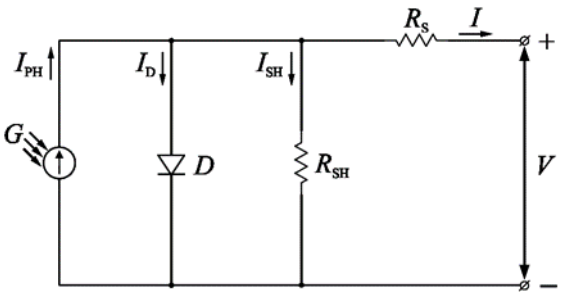

FIGURE 2. The equivalent circuit of the solar cell.

Normally, a PV array comprises N_P parallel branches, each with N_S solar cells in series. The total current from these modules can be described as [7]:

$$I = N_P \cdot I_{PH} - N_P \cdot I_0 \cdot \left[\exp\left(\frac{q(V + I \cdot R_S)}{N_S \cdot A \cdot k \cdot T}\right) - 1\right] - \frac{V + I \cdot R_S}{R_{SH}} \quad (2)$$

where I is the PV current, and V is the PV voltage.

Equation (2) comprises five unknown parameters (I_{PH}, I_0, A, R_S, R_{SH}), which are dependent on the surface temperature and solar irradiance of the PV array. In addition, one can solve (2) for the open-circuit voltage V_{OC} by setting $I = 0$, which means that no output current, whereas the short circuit current is obtained when the $V = 0$. Furthermore, the maximum power can occur when the product of the operating voltage V_{MPP} and current I_{MPP} is maximum.

This paper uses the mathematical model of the PV panel, as explained in detail in [31]. The model of the PV panel is implemented as a subsystem in Matlab/Simulink. The input variables of the model are the values of solar insolation and the surface temperature of the PV array, and the output variables are represented as the voltage and the current at the PV terminals.

B. THE BATTERY MODEL

Olivier Tremblay and Louis-A. Dessaint proposed a method to model the battery [32], [33]. The proposed model is based on the generalized shepherd's relation and is given by [32], [33]:

$$V_{batt} = E_0 - R \cdot i - K \cdot Q \Big/ \left(Q - \int idt\right) + A \cdot \exp\left(-B \cdot \int idt\right) \quad (3)$$

where $\int idt$ is the actual battery charge (Ah), R is the internal resistance (Ω), and Vbatt is the battery voltage (V), i is the battery current (A), A is the coefficient that characterizes the magnitude of the voltage drop during the exponential discharge zone (V), whereas B characterizes the inverse value of the capacity of the battery at the end of the exponential discharge zone (Ah)-1. K is the polarization resistance (Ω).

Considering (3), one may notice that the voltage is uniquely determined by the actual level of battery charge (SOC). Therefore, this model gives accurate results and represents the behavior of the battery. It can be reported that the main types of batteries available today include lead-acid, nickel-cadmium, nickel hydride, and lithium. The parameters of equation (3) are determined by the discharge characteristic of the battery, given by the manufacturer.

In the Simulink platform, the battery is modeled using a controlled voltage source connected in series with a constant resistance [31]. Besides, the model is made in the form of a separate subsystem with the possibility of entering the main parameters through a dialog box, which makes it easy to modify and use it. Thus, it helps in studying the characteristics

of different types of batteries, as well as to build models of batteries that are part of the PV system of any configuration.

C. DC-DC BUCK CONVERTER MODEL

The model of DC-DC converters has been built in Matlab/Simulink environment. The converter elements are interconnected with each other in Matlab platform according to the standard electrical scheme of the buck converter that is shown in Fig. 3.

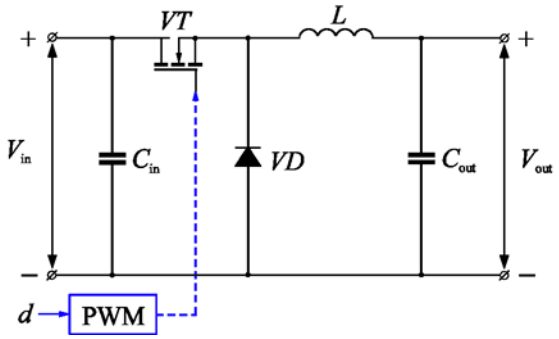

FIGURE 3. Schematic diagram of the DC-DC buck converter.

The power source to the converter is the PV panels. The output terminal of the converter is connected to a battery and a resistor simulating the load of the PV system. The control signal of the transistor switch (*VT*) is supplied from the PWM generator and is generated based on the duty cycle values d calculated by the MPPT controller.

The parameters of semiconductor devices (*VT*, *VD*) and elements of the converter (L, C_{in}, C_{out}) are determined at the design stage in accordance with the given values of power and the input and output voltage ranges that providing continuous conduction modes and reasonable output voltage ripple.

D. MAXIMUM POWER POINT CONTROLLER

In order to achieve an optimal power transfer, from the generator to load, it is imperative to maintain both the PV generator and the load at their respective optimum operating conditions. The main function of the tracker is the implementation of its MPPT algorithm, which provides the extraction of the maximum available power from the PV array.

In addition, to determine the values of d, which is utilized to drive the buck converter. In this paper, the search for MPP of the PV panels is carried out using the PSO algorithm. The PSO program code is implemented based on equations (4)-(9), in a separate m-file, which gives us the possibility to make the necessary changes in it. Furthermore, allowing us to investigate the effectiveness of the PSO at various values of its main parameters (w, c_1, c_2).

III. PARTICLE SWARM OPTIMIZATION

James Kennedy and Russell Eberhart created PSO algorithm in 1995, one of intelligence optimization tools based on the behavior of folk of birds [32]. The PSO is based on the continuous movement of particles in a possible solution space, while each particle in the search space is characterized by two variables: the coordinate x_i^k and the speed of movement v_i^k. In this algorithm, the position and the velocity of each particle of the swarm can be determined by the vectors:

$$X_i^k = \left[x_i^1, x_i^2, ..., x_i^{k_{\max}}\right] \quad \text{and } V_i^k = \left[v_i^1, v_i^2, ..., v_i^{k_{\max}}\right].$$

During the search process, the objective function is calculated, the position of a particle is influenced by the best particle in a neighborhood $Ppbest_i$. After that, the best solution passed by all particles *Pgbest* is selected, which simulates the instant exchange of information between particles. One of the significant disadvantages of the classical PSO in solving the optima local problems is that it is trapped in an unrequired solution, which leads to the loss of the exploration abilities [32], [33]. The modified PSO was proposed by Yuhi Shi and Russell Eberhart in 1998 [33] to overcome the drawbacks in the classical PSO. In this algorithm, unlike the classical algorithm, an additional coefficient of inertia w is used, which determines the gradient of change in the particle velocity. The modified PSO is described by the following equations [33]:

$$\begin{aligned} v_i^{k+1} &= v_i^k \cdot w + c_1 \cdot r_1 \cdot \left[Ppbest_i - x_i^k\right] + c_2 \cdot r_2 \cdot \left[Pgbest - x_i^k\right] \\ x_i^{k+1} &= x_i^k + v_i^k; \quad i = 1, 2, ..., N; \; k = 1, 2, ..., k_{\max} \end{aligned} \tag{4}$$

where c_1 and c_2 are the acceleration constants. r_1 and r_2 are random values in the range [0, 1]. i denotes the order number of the particle, and k denotes the number of the current iteration value. N is the number of the particles. $k_{\max}$ denotes the maximum number of iterations, and w denotes the coefficient of inertia.

To implement the PSO in the MPPT controller, the position of the particle x_i^k has been represented with the duty cycle d of the DC-DC buck converter. The value of d is updated by Δd with the speed of the particle v_i^k after a certain sampling time ts, and the PV system output power is considered to be the fitness function P_{PV}. The main parameters of the PSO (w, c_1, c_2) have a direct impact on its characteristics, and to achieve maximum efficiency of the algorithm, it is necessary to find the best combination of parameters. It is noticed that it is possible to use not only different numerical values of the parameters but also a variety of laws of change to select the optimal parameters of the controller. Moreover, the search for the best combination requires a significant number of simulations and is considered a difficult task. Evidence that this problem has no final solution to date confirms the results of studies, which offer different numerical values of the parameters of the PSO and the laws of their change [20], [21], [23], [26].

A. VARIABLE COEFFICIENTS PSO (VCPSO)

Based on a preliminary analysis and a generalization of the results of studies that utilized the PSO in MPPT control units, in this work, two modified versions of PSO were selected as analytical objects, which showed high MPP tracking efficiency of PV panel [17], [21], [41]. One of these

modifications is the variable coefficients PSO (VCPSO), proposed by the authors of [21].

Liu et al. suggested using VCPSO with the linear decreasing scheme for w [21].

$$w^k = w_{\max} - \frac{k}{k_{\max}} \cdot (w_{\max} - w_{\min}) \tag{5}$$

In the range from $w_{\max} = 1.0$ to $w_{\min} = 0.1$. Moreover, they proposed multidirectional laws and linear changes in c_1 and c_2.

$$\begin{aligned} c_1^k &= c_{1\max} - \frac{k}{k_{\max}} \cdot (c_{1\max} - c_{1\min}), \\ c_2^k &= c_{2\min} + \frac{k}{k_{\max}} \cdot (c_{2\max} - c_{2\min}) \end{aligned} \tag{6}$$

The upper and lower bounds of change c_1 and c_2 were set in the following range: $c_{1\min} = c_{2\min} = 1.0$ and $c_{1\max} = c_{2\max} = 2.0$.

The results of theoretical [21] and experimental [17] studies have shown that VCPSO with these proposed parameters provides effective tracking of the MPP of PV panels, consisting three series modules per string.

B. CONSTRICTION FACTOR BASED PSO (CFPSO)

On the other hand, another modification of the PSO, which has good prospects for applying for MPP trackers. This version was presented by Maris Clair and James Kennedy in 2002 [40]. The second technique that was named by constriction factor based PSO (CFPSO), the convergence of the algorithm is ensured by using a special constriction coefficient CF, the numerical values of which are demonstrated by the following equation:

$$CF = \frac{2}{\left|2 - \varphi - \sqrt{\varphi^2 - 4 \cdot \varphi}\right|}, \quad \text{where } \varphi = c_1 + c_2,\ \varphi > 4 \tag{7}$$

The new coordinates of the particle (i.e., the duty cycle d of the DC-DC converter) at each iteration of the algorithm are calculated by the equation:

$$d_i^{k+1} = d_i^k + CF \cdot \begin{bmatrix} d_i^k + c_1 \cdot r_1 \cdot \left(Ppbest_i - d_i^k\right) \\ + c_2 \cdot r_2 \cdot \left(Pgbest - d_i^k\right) \end{bmatrix} \tag{8}$$

The application of CFPSO algorithm guarantees the convergence of the algorithm for any values of c_1 and c_2, which greatly simplifies the task of determining their optimal values. The results of [41] confirms the possibility of using CFPSO for extracting the MPP of the PV system. Furthermore, preliminary studies have shown that the highest efficiency of the CFPSO algorithm in tracking the MPP is observed at the following numerical values $c_1 = c_2 = 2.5$, which corresponds to $CF = 0.382$.

Fig. 4 illustrates the flowchart of the searching mechanism by the modified PSO-based tracker. After finishing all iterations, the condition for reinitializing the algorithm will be

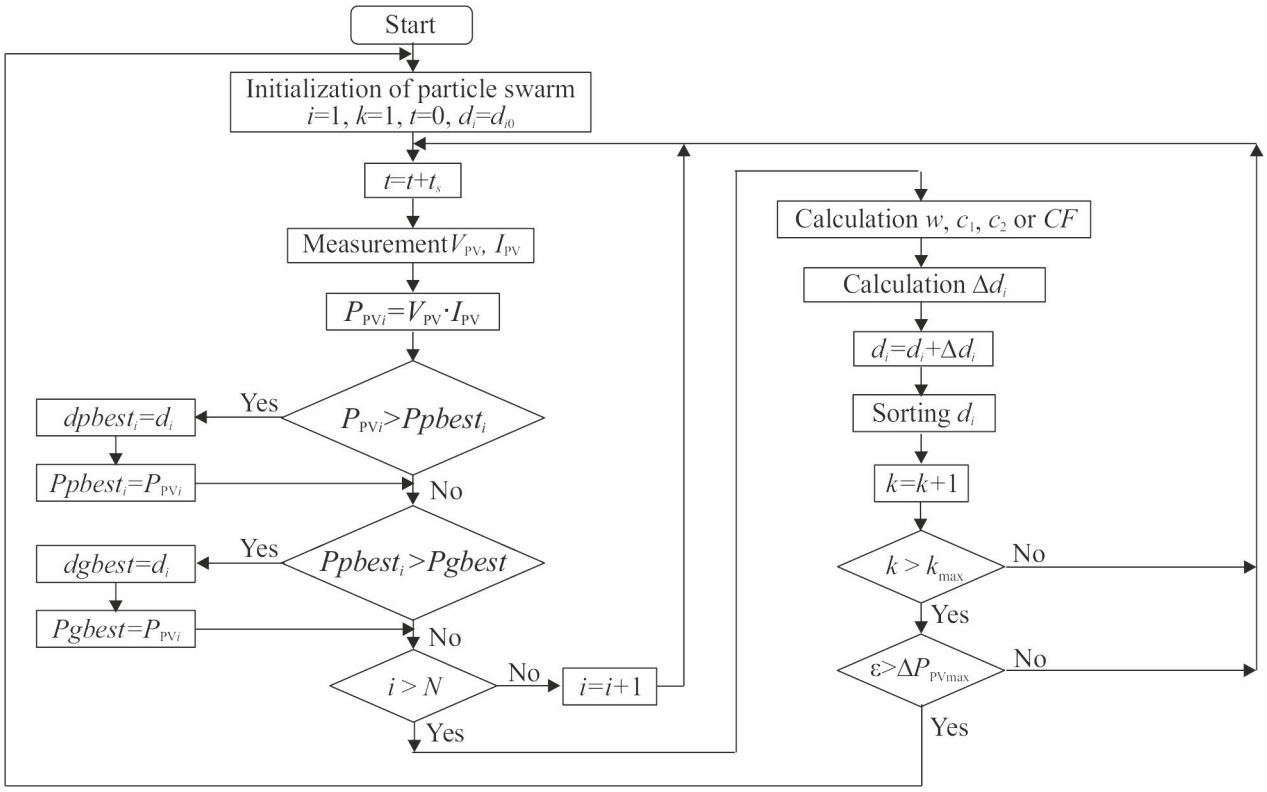

FIGURE 4. Flowchart for the searching mechanism by the modified PSO-based tracker.

checked. The condition for restarting the PSO algorithm is to change the output power of the PV panels by an amount greater than the set limit value:

$$\varepsilon = \frac{P_{\mathrm{PV}}^{k_{\max}} - P_{\mathrm{PV}}^{k_{\max}-1}}{P_{\mathrm{PV}}^{k_{\max}-1}} \cdot 100 > \Delta P_{\mathrm{PVmax}}(\%) \tag{9}$$

where $\Delta P_{\mathrm{PVmax}}$ is the specified limit value of the change in the PV output power over time *ts*.

In this study, the value of $\Delta P_{\mathrm{PVmax}}$ is assumed to be 5%, which provides a good compromise between the obtained and lost energy by tracking the MPP.

A distinctive feature of the proposed algorithm used in this work in comparison with standard PSO algorithms is the use of particle sorting, which will help in reducing the voltage stress on the power switch of the DC-DC converter and provides a reduction in the ripple of the output power of the PV array.

IV. SELECTION OF THE COMPONENTS OF THE AUTONOMOUS PHOTOVOLTAIC PLANT

In practice, the main task of designing a stand-alone PV system is to choose the size of the battery storage capacity. To get an accurate and optimal design, usually, the value of the average daily load consumption E_{L} can be used with the worst solar insolation conditions.

It is clear that the numerical value of E_{L} (kW/h) depends on the number and type of the power loads of a particular power plant and is determined individually for each PV system [36]. The size of the PV array can be evaluated as follows [37]:

$$A_{\mathrm{PV}} = \frac{E_{\mathrm{L}}}{H_{\mathrm{avg}} \cdot \eta_{\mathrm{PV}} \cdot T_{\mathrm{CF}}}, \tag{10}$$

where H_{avg} is the average solar insolation per day in kWh/day, η_{PV} is the efficiency of PV module in %, and T_{CF} is the temperature correction factor in %/°C.

It can be observed that the storage capacity of the battery Q_{BB} (kWh) is determined by taking into consideration the possible number of cloudy hours T_{BB} (h). the allowable depth of discharge for the battery bank (%), and the overall efficiency of the energy storage system η_{BB} (taking into account the efficiency of the battery and the output inverter):

$$Q_{\mathrm{BB}} = \frac{E_{\mathrm{L}} \cdot T_{\mathrm{BB}}}{24 \cdot DOD \cdot \eta_{\mathrm{BB}}} \tag{11}$$

In this work, the autonomous PV power plant is considered as an object of research, which comprises 3 PV modules Kyocera Solar KD320GX-LPB connected in series and 4 batteries MONBAT 12 MVR200 with a total capacity of 9.6kWh. Table 1 listed the electrical parameters of the Kyocera Solar KD320GX-LPB PV module while the table 2 has the technical specifications of the battery MONBAT 12 MVR200 [30].

In order to select the parameters of the DC-DC converter, it is necessary to set the operating range of its input voltage (i.e., PV side), which is determined by the values of the irradiance G and the temperature of the PV modules. This study considers the following ranges of changes in external climatic conditions: irradiance $G = 100 - 1000$ W/m^2 and temperature $T_{\mathrm{FM}} = -25 - 50$°C.

Fig. 5a demonstrates the electrical voltage-power characteristics of the PV module under the given values of $G = 100$, 400, 700, 1000 W / m^2 and $T_{\mathrm{FM}} = -25$, 0, 25, 50 °C. The shaded area in Fig. 5a represents the operating range of the input voltage of the DC-DC buck converter.

TABLE 1. Electrical parameters of the Kyocera solar KD320GX-LPB PV module.

Parameters	Values
Open-circuit voltage, V_{OC} (V)	49.5
Short circuit current, I_{SC} (A)	8.6
Voltage at *Pmax*, V_{MPP} (V)	40.1
Current at *Pmax*, I_{MPP} (A)	7.99
Maximum power, P_{MPP} (W)	320.4
Open circuit voltage coefficient V_{OC}, k_{V} (V/°C)	-0.1832
Short circuit current coefficient I_{SC}, k_{I} (A/°C)	0.00328
Number of cells connected in series, N_{S}	72

TABLE 2. The technical specifications of the battery MONBAT 12 MVR200.

Parameters	Value
Battery type	Lead-acid Maintenance-free, AGM technology
Rated voltage (V)	12
Number of elements (PCs.)	6
Internal resistance (IEC 60896-21/22) (Ω)	3,89
Short circuit current (IEC 60896-21/22) (A)	3200
Weight (Kg)	61

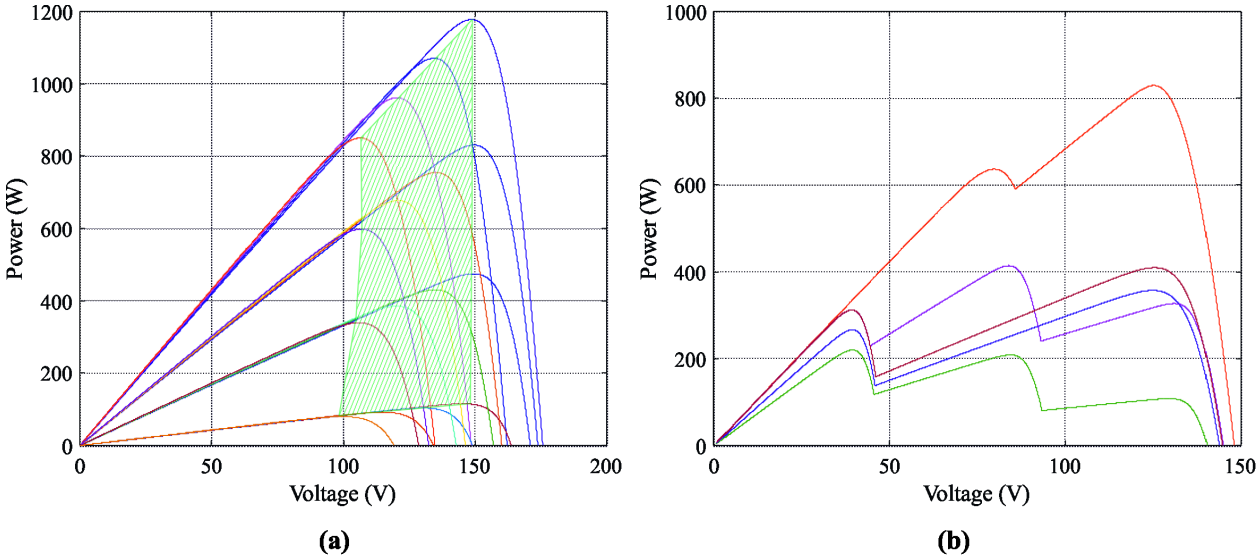

FIGURE 5. Voltage-power characteristic curves for the Kyocera solar PV module: a) under normal conditions and b) under PSC.

As it can be seen from Fig. 5a, the required buck converter in the proposed model should have the following operating power characteristics: a rated power of $P_{\text{nom}} = 1200$ W and input voltage in the range of $V_{\text{in}} = 98 - 148$ V.

It can be observed that the operating range of the input voltages and the rated power of the DC-DC converter can be easily evaluated analytically, using the given data of the technical specification of the PV module, and assuming that when the climatic conditions change, the MPP voltage (V_{MPP}) will change proportionally to the open-circuit voltage, and the MPP current (I_{MPP}) also will change proportionally to the photocurrent. Mathematically, the following equations can be used to determine V_{MPP} and I_{MPP} at arbitrary values of G and T_{FM} [30]:

$$I_{\text{MPP}} = \left[I_{\text{MPP\_STC}} + k_I \cdot (T_{\text{FM}} - T_{\text{STC}})\right] \cdot N_{\text{FMp}} \cdot \frac{G}{G_{\text{STC}}} \quad (12)$$

$$V_{\text{MPP}} = \left[V_{\text{MPP\_STC}} + k_V \cdot (T_{\text{FM}} - T_{\text{STC}})\right] \cdot N_{\text{FMs}} - \left[(I_{\text{MPP\_STC}} - I_{\text{MPP}}) \cdot R_S\right] \cdot \frac{N_{\text{FMs}}}{N_{\text{FMp}}} \quad (13)$$

where $V_{\text{MPP\_STC}}$ and $I_{\text{MPP\_STC}}$ are the MPP voltage and the MPP current respectively of the PV module at the standard test condition (STC: $G_{\text{STC}} = 1000$ W/m^2, $T_{\text{STC}} = 25$°C), N_{FMs} and N_{FMp} are the number of series and parallel connected PV modules, and R_{S} is the series resistance of the PV module.

The value of R_{S} is calculated by (14) [30]:

$$R_S = \frac{\frac{N_S A \cdot k T_{\text{STC}}}{q} \cdot \ln\left(1 - \frac{I_{\text{MPP\_STC}}}{I_{\text{SC\_STC}}}\right) + V_{\text{OC\_STC}} - V_{\text{MPP\_STC}}}{I_{\text{MPP\_STC}}} \quad (14)$$

where N_{S} is the number of the series-connected solar cell of PV modules.

From the above analysis, it is obvious that the maximum power of the PV panel can be obtained at $G = 1000$ W/m^2, $T_{\text{FM}} = -25$° C whereas the minimum power of the PV module can be determined at $G = 100$ W/m^2, $T_{\text{FM}} = 50$ °C. Furthermore, the following parameters for the designed PV system can be calculated from equations (12)-(14) (at $R_{\text{S}} = 0.38\Omega$):

- Minimum mode: $V_{\text{MPP}} = 98.4$ V; $I_{\text{MPP}} = 0.81$ A; $P_{\text{MPP}} = 79.4$ W;
- Maximum mode: $V_{\text{MPP}} = 147.6$ V; $I_{\text{MPP}} = 7.83$ A; $P_{\text{MPP}} = 1155.1$ W.

It can be cleared that the comparison of the results of calculations of V_{MPP} and I_{MPP} obtained by equations (12)-(14) with the results of these values obtained from the dynamic simulation of the PV characteristics (Fig. 5a) showed that the maximum error in determination of V_{MPP} and I_{MPP} was not more than 4% between the two methods. According to these results, one can claim that the simplified proposed approach for determining the parameters of the modes of MPP of the PV panels provides sufficiently high accuracy. In addition, the proposed method for determining the parameters of the modes of the MPP of the PV array provides reliability in determining the operating range of the input voltage of the DC-DC converter under uniform solar irradiance of the PV string; however, it does not take into consideration the possible modes of PSC of the PV panels.

Fig. 5b illustrates the power-voltage characteristic of the PV array under the PSC. From Fig. 5b, it can be observed that the characteristics of the PV module have a more complex shape with several local peaks ranging from one to N_{FMs} and only one global peak [9], [10].

It should be noted that PSC often occurs in the PV system and in order to obtain the most efficient use of the solar power, the possible modes of the PSC must be considered to

determine the operating range of the input voltage of the DC-DC converter. Consequently, to determine the value of V_{MPP} in the minimized mode, one can use the same equations (12)-(14), by assuming $N_{FMs} = 1$.

Taking into account the PSC, the minimum mode parameters are defined as follows:

– Minimum mode: $V_{MPP} = 32.8$ V; $I_{MPP} = 0.81$ A; $P_{MPP} = 26.5$ W.

In general, the obtained value of the V_{MPP} voltage defines the value of the output voltage of the DC-DC converter and the boundaries of its duty cycle. Thus, the output voltage V_{out} of the buck converter can be selected from the relation:

$$V_{out} < V_{MPP(min)} \tag{15}$$

A value of $V_{out} = 24$V is chosen in this paper, and then the boundary values of the duty cycle will be calculated as follows:

$$\begin{aligned} d_{min} &= \frac{V_{out}}{V_{MPP(max)}} = \frac{24}{147.6} = 0.16, \\ d_{max} &= \frac{V_{out}}{V_{MPP(min)}} = \frac{24}{32.8} = 0.73 \end{aligned} \tag{16}$$

It can be noticed that the maximum power of the PV panel will occur when the equivalent resistance of the MPP R_{MPP} and the equivalent input resistance of the DC-DC converter R_{in} are equal. Furthermore, the value of R_{MPP} depends on the climatic conditions and varies in a wide range. The limiting values of R_{MPP} can be calculated by (17).

$$\begin{aligned} R_{MPP(min)} &= \frac{V_{MPP(max)}}{I_{MPP(max)}} = \frac{147.6}{7.83} = 18.9\Omega, \\ R_{MPP(max)} &= \frac{V_{MPP(min)}}{I_{MPP(min)}} = \frac{98.4}{0.81} = 121.5\Omega \end{aligned} \tag{17}$$

The value of R_{in} depends on the topology of the converter, its connected load R_{out}, and the value of d.

Basically, when searching for the MPP, the controller changes the value of d so that the condition of $R_{MPP} = R_{in}$ is fulfilled. If we consider that we have an ideal DC-DC converter ($P_i = P_o$), then an important practical relation can be derived:

$$\frac{V_{MPP}^2}{R_{MPP}} = \frac{V_{out}^2}{R_{out}} = \frac{(V_{MPP} \cdot d)^2}{R_{out}} \Rightarrow d = \sqrt{\frac{R_{out}}{R_{MPP}}} \tag{18}$$

Since the duty cycle cannot accept any value outside the interval [0, 1], it can be observed from (18) that in order to ensure the PV array is operating in the MPP mode, the output resistance of the DC-DC buck converter must be less than the minimum equivalent resistance of the PV array at MPP:

$$R_{out} < R_{MPP(min)} \tag{19}$$

If the connected load of the buck converter is the battery, then condition (19) is easily satisfied since the internal resistance of the battery, in this case, is less than 1 Ω (Table 2).

In most practical cases, the DC-DC converter is designed to operate in continuous current operation (CCO), which ensures its better controllability and minimization of energy losses. CCO is provided by choosing the appropriate filter inductance L, the value of which for the buck converter is given by [38]:

$$L > \frac{V_{out} \cdot (1 - d)}{2 \cdot I_{out} \cdot f} \tag{20}$$

where $f = 1/T$ is the switching frequency, I_{out}, V_{out} are the output current and voltage respectively of the converter.

To save CCO up to the minimum load current, equation (20) can be defined in an alternative way as:

$$L > \frac{V_{out} \cdot d_{max} \cdot (1 - d_{max})}{2 \cdot I_{MPP(min)} \cdot f} \tag{21}$$

Substituting the calculated data of the minimum mode in equation (21) and taking $f = 25$ kHz, the calculated value of the inductance of the filter under consideration will be $L = 116.8\mu$H, and value of $L = 120\mu$H is chosen in this study.

The main purpose of designing the output capacitor C_{out} is to limit the amount of ripple in the output voltage ΔV_{out} to the desired value. When working on a passive load, this condition for the buck converter is formulated in the form of equation (22) [38]:

$$C_{out} > \frac{V_{out} \cdot (1 - d)}{8 \cdot \Delta V_{out} \cdot L \cdot f^2} \tag{22}$$

It should be noted that if the load of the converter is the battery, it is not necessary to use the output capacitor since the battery has its own large capacitor. Basically, a mandatory element of the DC-DC converter is the input capacitor C_{in}, which provides a smoothing of the ripples of the output voltage of the PV array due to the nonlinearity of its characteristics [39]. The selection of the input capacitor C_{in} is based on the condition of limiting the value of the fluctuations in the input voltage of the converter to the required values (usually 1-5%), determined by a given voltage ripple factor γ_{Vin} at the power operating point:

$$C_{in} > \frac{d \cdot (1 - d)}{8 \cdot \gamma_{Vin} \cdot L \cdot f^2} \tag{23}$$

It can be noted that when determining the value of C_{in} in equation (23), it is necessary to substitute d_{min} corresponding to the maximum value of the input voltage. In these studies, it was assumed that $C_{in} = 25\mu$F, which will ensure a reduction in the ripple of the input voltage in all possible operating modes to a level below 1%.

V. SELECTION AND OPTIMIZATION OF PARTICLE SWARM ALGORITHM PARAMETERS

A. THE SELECTION OF THE SAMPLING TIME

This section presents the selection and the design of the sampling time t_s for the control unit of the MPPT of the PV array. Initially, t_s is considered as one of the main parameters which control the convergence speed of the PSO algorithm in extracting the GMPP of the PV string. It can be noted that with small values of t_s, the tracking time of GMPP

can be reduced, but this may lead to fluctuations around the MPP, and as a consequence to a decrease in the tracking accuracy. In order to select the optimal step size of the PSO algorithm based MPPT, a new method is suggested to select the minimum optimum value of the t_s, in which the amount of transient process will end in searching for the MPP of the PV string. In general, the transient process is initiated when a change in the duty cycle of the converter is experienced by the value of Δd. The choice of the optimal ts value must be made, taking into account the topology and the values of the power filter parameters of the converter, which determine its dynamic properties. To determine the dynamic characteristics of a nonlinear impulse system, it is convenient to use methods of analysis based on continuous models of converter devices. A simplified equivalent of a continuous linearized model of a buck converter (Fig. 3), which is connected to a battery; can be represented in the form of a circuit as shown in Fig. 6.

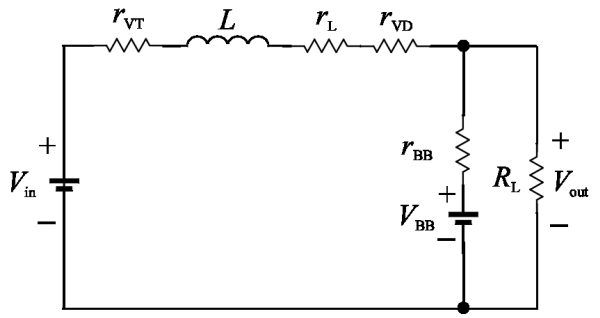

FIGURE 6. Schematic of the continuous linearized model of a buck connected to a battery.

In the simplified model of the converter, the battery bank is represented as a non-inertial link consisting of a series-connected voltage source with a value of V_{BB} equal to the nominal voltage of the battery, and the active resistance r_{BB} equal to its equivalent internal resistance. The value of r_{BB} depends on the configuration of the battery. The technical specifications of the bank of battery are used and can be found by equation (24):

$$r_{BB} = \frac{N_{batt.s}}{N_{batt.p}} \cdot r_{batt} \tag{24}$$

where $N_{batt.s}$ and $N_{batt.p}$ are the number of series-connected and parallel-connected batteries respectively in the battery bank, and r_{batt} is the internal resistance of the battery according to the technical specifications.

In the considered PV system configuration, the proposed battery bank comprises 2 series and 2 parallel connected MONBAT 12 MVR200 batteries, and the evaluated value of the internal resistance is $r_{BB} = 3.89\Omega$.

It can be noted that the value of the load resistance can be neglected, due to the fact that $r_{BB} \ll R_L$. The time constant of the buck converter τ, loaded on the bank of battery is determined using the following expression:

$$\tau = \frac{L}{d_{nom} \cdot r_{VT} + (1 - d_{nom}) \cdot r_{VD} + r_L + r_{BB}} \tag{25}$$

where r_{VT}, r_{VD} and r_L are the equivalent active resistances of the transistor switch, diode, and inductor, respectively.

It should be noted that the duration of any transition process is equal (3-5) τ. In this study, it is recommended to use $t_s = 3\tau$ as the optimal value of t_s, which will provide the maximum speed of tracking the MPP of the PSO. Also, it will provide a stable operation in extracting the MPP of the PV array. It can be noted that the analysis of equation (25) shows that the parameters which effect on the value of t_s are the values of the active and inductive resistance of the inductor.

For the assumed constant values $d_{nom} = 0.5$, $r_{VT} = r_{VD} = 0.01\Omega$, $r_{BB} = 3.89\Omega$ and $L = 120\mu$H. The calculated value of ts will be as follows: at $r_L = 0.01\Omega$, $t_s = 0.015$s and at $r_L = 0.1\Omega$, $t_s = 0.0032$s.

To verify the accuracy of the proposed method which is used for determining the optimal value of the t_s, in this paper, a series of simulations were carried out to study the dynamic characteristics of the buck converter connected to the battery bank, powered from an ideal voltage source. In the selected model, the dynamic characteristics of the buck converter connected to the battery bank and the above-defined parameters are used. Considering the output power P_{out} as the response of the model and the change in the duty cycle by Δd as the perturbations affect the model, the results of the simulation of transient changes in the output power of the DC-DC converter for three different values of r_L are demonstrated in Fig. 7. From Fig. 7, it can be visualized that the change of Δd is chosen to give the output response of the value $\Delta P_{out} = 1000$ W in all test cases.

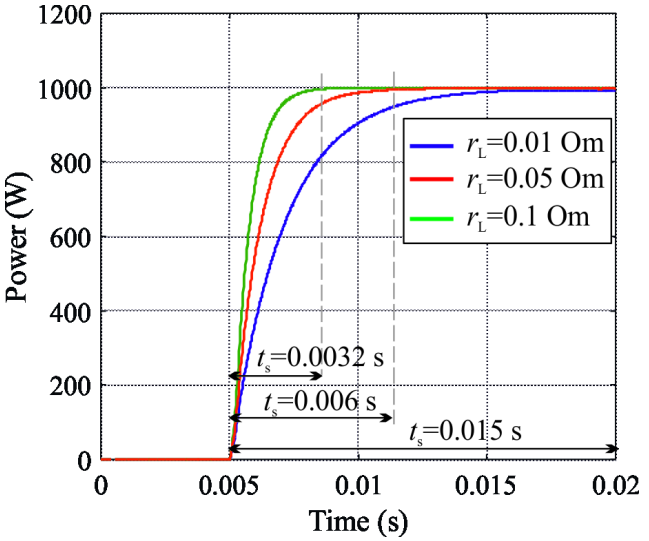

FIGURE 7. The simulation results of the transient changes in the output power of the buck converter connected to the battery bank.

A comparison of the numerical values of t_s calculated by the proposed method and those obtained as a result of dynamic modeling shows a good agreement of the results, which indicates the possibility of using this approach to select the optimal values of t_s.

One can drive that, the comparison of the obtained numerical values of the calculated t_s by the proposed method and this which is derived from the simulations of the dynamic characteristics; the robustness and accuracy of the proposed method in determining the t_s, which indicates the possibility of using this approach to select the optimal values of the t_s. In this work, the values of the parameters of the converter elements ($r_{VT} = r_{VD} = 0.01\Omega$, $r_L = 0.1\Omega$) are used, typical values for the considered stand-alone PV system, for which the value $t_s = 0.004$s is taken as the optimal value of the sampling time.

B. THE SELECTION OF THE NUMBER OF PARTICLES AND THE NUMBER OF ITERATIONS

It can be observed that the important parameters of PSO controller are the number of particles N and the maximum number of iterations k max. A large number of N provides a comprehensive scan of the search area, but this will lead to an increase in the tracking time of the GMPP of the PV array.

By applying the PSO to search for GMPP of the PV panels, there is no need to use a large number of N, which is utilized for extracting the global extremum of complex nonlinear functions Griewank, Rastrigin, Rosenbrock, etc., as a rule; N is less that than 10. From the practical point of view, the select of the optimal value of N depends not only on the parameters of (w, c_1, c_2) but also on the shape of the power-voltage curve of the PV array, which in turn is determined by the PV array configuration and other external factors having a stochastic nature. Under these conditions, the use of analytical calculation methods is impossible; while the optimal number N can be only found based on the results of mathematical modeling or experimental studies.

It can be noticed that in most of the scientific researches related to the study of the PSO, the N and k max are chosen together with the algorithm's parameters for one specific configuration of the PV panel, which can limit the practical scope of the obtained results. This work aims to determine the relationship between the number of particles and the efficiency of the PSO algorithm, taking into account the configuration of the PV string. To clarify the proposed claim and observation, let us consider three different configurations of the PV string, as illustrated in Table 3.

TABLE 3. The proposed different configurations of the PV array.

Label	Parameters	P_{max}, W
PV1	3 series-connected PV Kyocera Solar KD320GX-LPB modules	960
PV2	4 series-connected PV Kyocera Solar KD250GX-LPB modules	1000
PV3	8 series-connected PV Kyocera Solar KD130GX-LP modules	1040

The choice of these configurations is based on two factors: First, all the PV panels are made of identical solar cells, which ensures the identity of their characteristics. Second, each configuration has approximately the same power, which makes it possible to use the same DC-DC converter with the parameters defined above.

The different shading patterns for each configuration of the PV panel are shown in Table 4, and the voltage-power characteristics of these cases are demonstrated in Fig. 8.

The simulation results for the 10 cases have been performed with the number of particles N from 3 to 8. Two different modified versions of VCPSO and CFPSO with the defined parameters presented in section 2 have been employed in simulations as a controller of MPP. The simulation results for the first configuration (PV1) are illustrated in Table 5.

For achieving the accuracy of comparison, the number of iterations is chosen according to the recommendations of [21] and [17]; equal to $I_{max} = 30$, and remained unchanged in all computational processes. It can be noted that the maximum number of iterations and the number of particles determine the numerical values of the tracking time of the MPP of the PV string:

$$t_{MPP(max)} = k_{max} \cdot t_s = N \cdot I_{max} \cdot t_s \tag{26}$$

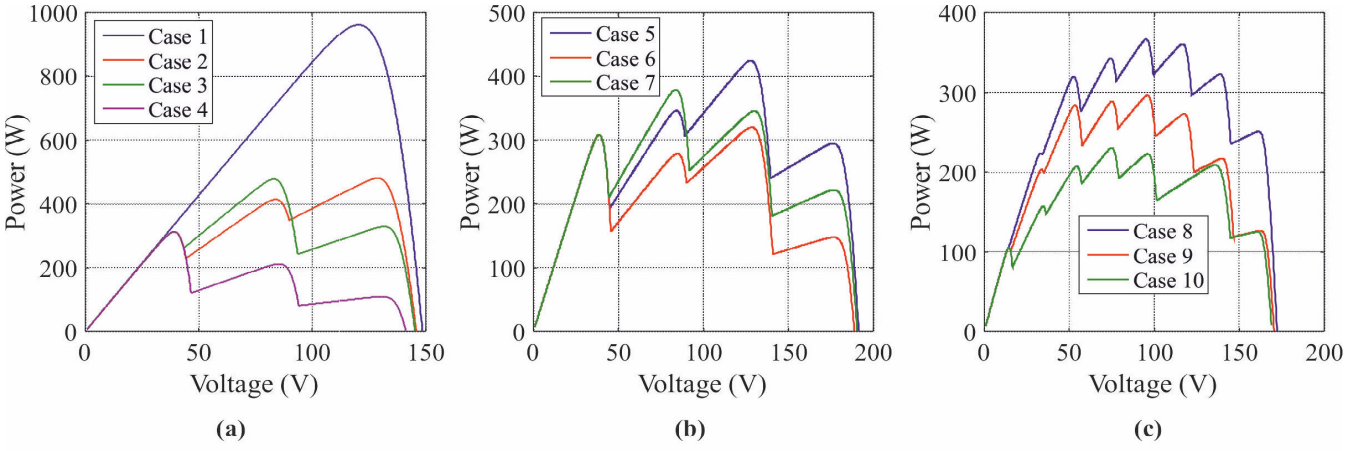

FIGURE 8. Power-voltage characteristics different cases of shading patterns of À) PV1, b) PV2, c) PV3.

TABLE 4. Different shaded cases for the proposed PV configurations.

Configuration	Case No.	Solar irradiance, G_i (W/m^2)								P_{MPP}, (W)	V_{MPP}, (V)	I_{MPP}, (A)
		G_1	G_2	G_3	G_4	G_5	G_6	G_7	G_8			
PV1	1	1000	1000	1000	–	–	–	–	–	961.2	120.2	8.00
	2	1000	600	450	–	–	–	–	–	481.1	128.8	3.74
	3	1000	700	300	–	–	–	–	–	478.6	82.8	5.78
	4	1000	300	100	–	–	–	–	–	312.3	38.5	8.10
PV2	5	1000	500	400	200	–	–	–	–	332.8	95.5	3.48
	6	900	400	300	100	–	–	–	–	250.8	95.9	2.62
	7	800	550	320	150	–	–	–	–	292.3	61.6	4.74
PV3	8	1000	900	800	600	500	400	300	200	365.8	95.3	3.84
	9	1000	800	700	500	400	300	200	100	295.6	95.3	3.10
	10	1000	600	500	400	300	200	200	100	230.0	74.6	3.08

TABLE 5. THE comparative results of the performance of the PSO technique with different number of particles.

Case No.	Number of particles N	Technique									
		VCPSO					CFPSO				
		P_{MPP}, W	V_{MPP}, V	η, %	t_{MPP}, s	E_{MPP}, J	P_{MPP}, W	V_{MPP}, V	η, %	t_{MPP}, s	E_{MPP}, J
1	3	961.2	120.2	100.00	0.25	61.2	956.6	117.7	99.52	0.14	33.8
	4	960.1	118.9	99.89	0.27	79.2	956.6	117.7	99.52	0.16	30.7
	5	961.1	119.3	99.99	0.38	81.8	957.3	117.9	99.59	0.26	41.8
	6	960.2	119.0	99.89	0.58	117.8	956.6	117.7	99.52	0.35	44.8
	8	961.0	121.6	99.98	0.82	183.1	957.0	117.8	99.56	0.52	63.4
2	3	410.9	81.8	85.41	0.22	45.0	478.6	126.6	99.48	0.20	15.3
	4	478.8	126.7	99.52	0.33	39.8	413.3	83.1	85.90	0.21	40.2
	5	481.1	128.5	100.00	0.41	40.3	478.6	126.6	99.48	0.36	22.3
	6	478.8	126.7	99.52	0.6	68.1	478.6	126.6	99.48	0.41	24.6
	8	478.6	126.7	99.49	0.94	95.9	479.2	127.0	99.61	0.52	29.2
3	3	476.7	82.4	99.60	0.24	31.8	476.0	81.9	99.46	0.20	11.5
	4	477.5	83.9	99.77	0.42	26.1	476.0	81.9	99.46	0.19	11.0
	5	476.1	83.7	99.48	0.38	39.7	476.0	81.9	99.46	0.24	14.7
	6	477.8	82.6	99.82	0.66	52.4	476.0	81.9	99.46	0.30	15.4
	8	476.9	82.6	99.65	0.78	51.9	476.2	82.0	99.50	0.46	20.6
4	3	312.3	39.0	100.00	0.18	5.7	311.7	39.1	99.81	0.13	3.1
	4	312.2	39.3	99.98	0.42	6.1	311.7	39.1	99.81	0.17	3.9
	5	312.3	38.9	99.98	0.52	11.5	311.7	39.1	99.81	0.19	7.0
	6	312.3	39.0	100.00	0.48	15.0	311.7	39.1	99.81	0.26	6.3
	8	312.2	39.3	99.98	0.94	18.2	311.7	39.1	99.81	0.32	11.4

where I_{max} denotes the maximum number of iterations for each particle ($k_{max} = N \cdot I_{max}$).

In this paper, the tracking efficiency of the MPPT algorithm is evaluated according to 3 indicators: the tracking efficiency η, the energy losses when searching for MPP E_{MPP}, and the actual tracking time of the MPP of the PV array t_{MPP}. The tracking efficiency of the controller is determined by equation (27).

$$\eta = \frac{P_{MPP}}{P_{MPP(max)}} \cdot 100, \% \tag{27}$$

where P_{MPP} is the value of output power of the PV string, that tracked by the controller, and $P_{MPP(max)}$ is the value of maximum available power. The energy loss can be expressed as:

$$E_{MPP} = \int_0^{t_{MPP(max)}} \left(P_{MPP(max)} - P_{MPP}^k\right) \cdot \mathrm{dt}, J \tag{28}$$

where P_{MPP}^k is the current values of the power of the PV panel in the search process of the MPP. The actual tracking time of the MPP of the PV array can be represented as:

$$t_{MPP} = \frac{\left|P_{MPP} - P_{MPP}^k\right|}{P_{MPP}} \cdot 100 < 1\% \tag{29}$$

As can be seen from Table 5, the VCPSO algorithm based on 3 and 4 particles provides better tracking efficiency and energy losses. However, the two controllers can be trapped around the local peak in some cases of studies. In other words, in the second test case, the VCPSO extracts the local peak at $N = 3$, whereas the CFPSO catches the local peak at $N = 4$. According to these simulation results, one can claim that with a large number of N, the energy loss and the tracking time will increase significantly, while the tracking efficiency does not improve. Furthermore, it cannot be guaranteed that the GMPP can be tracked with a large number of particles. It can be noted that in case 9, the CFPSO extracts the local peak at $N = 3$, 4, 6 and 8. From the analysis of the simulation results, one can drive that the minimum energy loss, and the high tracking efficiency of the controller can be provided only with four particles. Thus, in this paper, to achieve the optimal performance of the proposed algorithms based

TABLE 6. Detailed comparison of the proposed techniques under study.

Case No.	VCPSO				CFPSO			
	η, %	t_{MPP}, s	It_{MPP}	E_{MPP}, J	η, %	t_{MPP}, s	It_{MPP}	E_{MPP}, J
1	99.89	0.27	16.9	79.2	99.52	0.16	10.0	30.7
2	99.52	0.33	20.6	39.8	85.90	0.21	13.1	40.2
3	99.77	0.42	26.3	26.1	99.46	0.19	11.9	11.0
4	99.98	0.42	26.3	6.1	99.81	0.17	10.6	3.9
5	99.94	0.38	23.8	23.1	99.89	0.26	16.3	9.1
6	99.95	0.38	23.8	19.5	99.95	0.22	13.8	7.4
7	99.86	0.33	20.6	12.9	99.62	0.21	13.1	5.0
8	99.94	0.35	21.9	15.2	99.96	0.23	14.4	7.3
9	99.87	0.27	16.9	15.3	97.29	0.34	21.3	9.9
10	99.93	0.28	17.5	8.5	99.94	0.11	6.9	3.2
Average	**99.87**	**0.34**	**21.5**	**24.6**	**98.13**	**0.21**	**13.1**	**12.8**

trackers, the optimal number of particles is chosen to equal four particles. The second important task in this section is to determine the best controller that can be implemented in the control search unit for the GMPP of the PV panels. Table 6 presents a detailed comparison of the performance of the two proposed techniques in terms of tracking efficiency, energy loss, convergence speed (iteration), and tracking time for $N = 4$.

The number of iterations taken by each controller to reach the GMPP can be rewritten as:

$$It_{\mathrm{MPP}} = \frac{t_{\mathrm{MPP}}}{t_{\mathrm{MPP(max)}}} \cdot I_{\max} = \frac{t_{\mathrm{MPP}}}{N \cdot I_{\max} \cdot t_s} \cdot I_{\max} = \frac{t_{\mathrm{MPP}}}{N \cdot t_s} \tag{30}$$

As it can be seen from Table 6, the CFPSO based tracker is the best compared with VCPSO based tracker in terms of the number of iterations and the energy loss for all 10 studied cases. One can see that the CFPSO based controller can be trapped at the local peak as shown in case 2. Also, the VCPSO controller has the best tracking efficiency for all different studied cases compared to CFPSO based tracker. Therefore, the high tracking efficiency of the VCPSO compared to CFPSO urges us to utilize it in the control search unit for the GMPP under the uniform and PSC of the PV panels.

According to the simulation results, shown in Table 6, one can see that the convergence speed of the VCPSO controller for all test cases was between 17 to 24 iterations to get the GMPP of the PV panel when $I_{\max} = 30$. Therefore, one can say that the optimal maximum number of iterations for the controller can be equal $I_{\max} = 24$, in order to reduce the time tracking required by the controller to catch the GMPP under the PSC. The choice of this value will provide high speed and reliable tracking of the GMPP of the PV panel.

C. PARAMETERS INITIALIZATION

The initialization of the positions of the particles is essential for a successful search for the MPP. It can be noted that the coordinate of the MPP can be changed over a wide range with the changes in the external environmental conditions. It is necessary to arrange the particles throughout the search area uniformly. According to the MPP controller, the search area is limited to $d_{\min}$ and $d_{\max}$, the values of which should be used as the coordinates of the first and last particles in the first iteration. For the PV system investigated in this paper, the numerical values of $d_{\min}$ and $d_{\max}$ are defined in Section 4. Taking into account that the calculation of these values was carried out by a simplified method, without taking into account losses in the buck converter, thus it is advisable to determine the initial coordinates of the first and last particles with a certain margin: $d_1^1 = 0.1$, $d_1^N = 0.8$.

To determine the initial coordinates of the intermediate particles, it is convenient to use the following equation:

$$d_i^1 = d_i^1 + \frac{d_N^1 - d_1^1}{N - 1} \cdot (i - 1), \tag{31}$$

where i is the sequence number of the particle.

VI. SIMULATION RESULTS

This section aims to validate the correctness of the proposed methodology, which has been utilized to select the parameters defined in sections 3, 4 and 5 of the VCPSO based controller. All simulations in this study have been performed using a Matlab/Simulink tool. Fig. 9(a) shows the execution process of the proposed PSO based MPP tracker for the PV system. From the figure, the dynamic optimization algorithm has been applied to search the global MMP at each time step. Moreover, Fig. 9(b) illustrates the simulation model of the PV system using the Matlab platform. Furthermore, table 7 summaries the optimal selected parameters of the proposed PV System which has been applied in simulation.

TABLE 7. The optimal selected parameters of the proposed PV system.

The sample time (ts)	0.004 s
The maximum number of iterations (Imax)	24 iterations
L	120μH
C_{in}	25 μF
Number of particles(N)	4

To assess the effectiveness of the proposed VCPSO algorithm, the standard PSO (SPSO) proposed by the authors [25] is compared with the VCPSO tracker in this work. The SPSO is based on the following parameters: $N = 3$ particles,

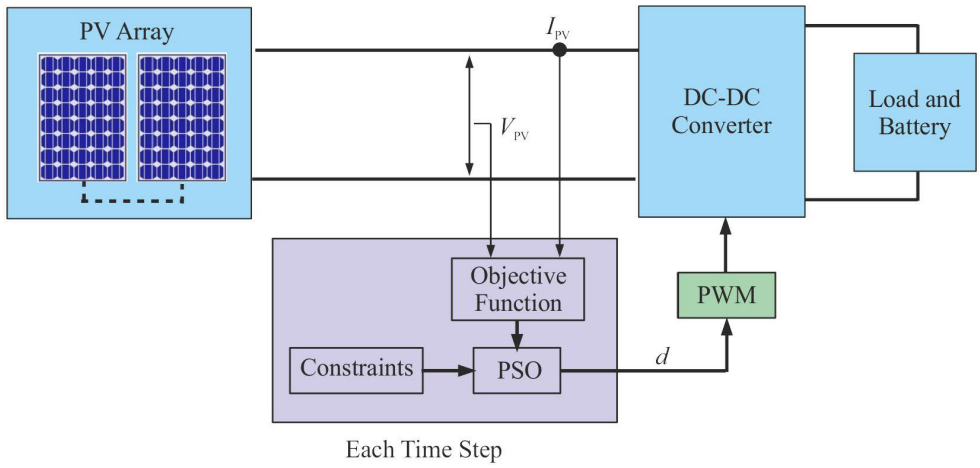

(a)

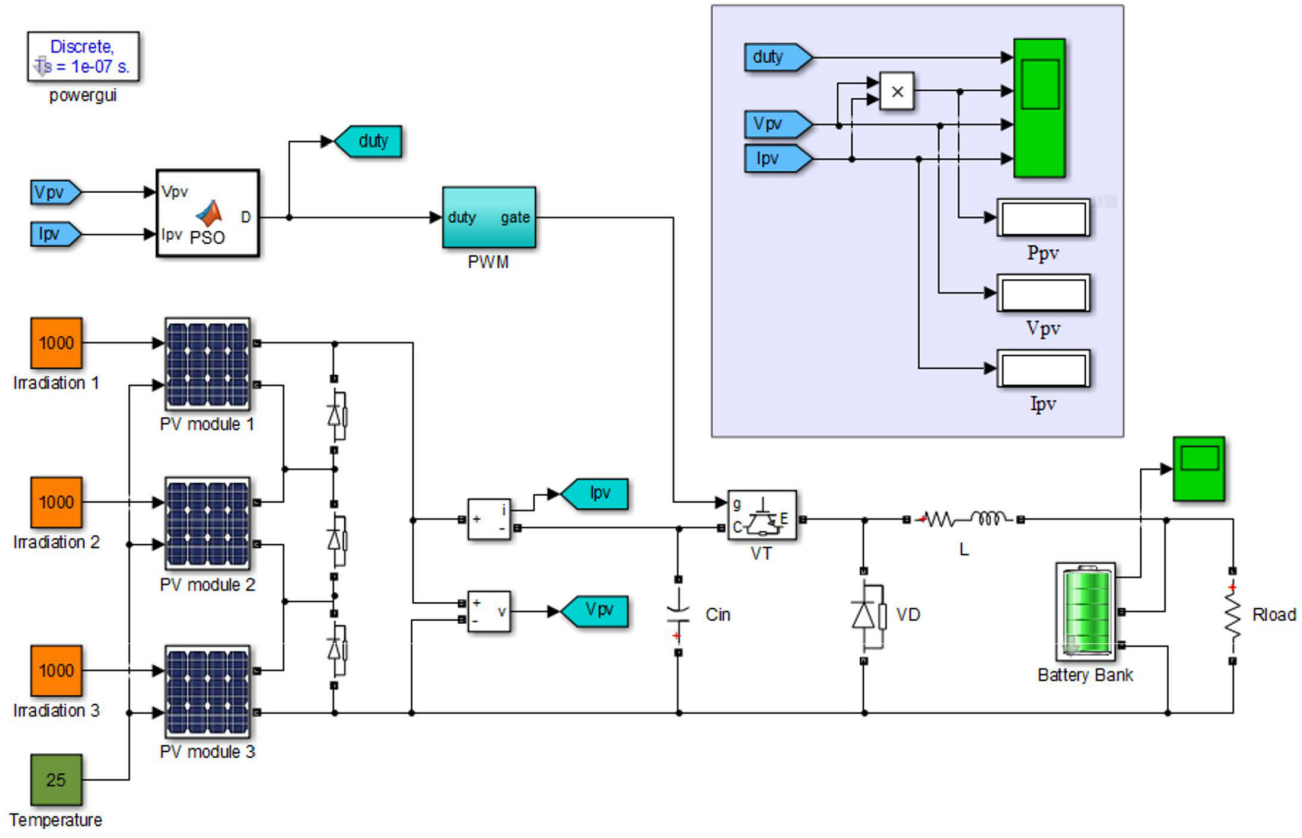

(b)

FIGURE 9. (a) Block diagram of execution of dynamic PSO optimization for MPPT of PV array (b) Matlab/Simulink of the proposed PV system.

$c_1 = 1$, $c_2 = 2$, and $w = 1$ [25]. To improve the convergence of the selected SPSO, the maximum value of the velocity vector (increment of the duty cycle) is limited by the value: $\Delta d_{\max} \leq 0.02$, recommended by the authors of [42]. For the proposed VCPSO, the values of the parameters that are defined in section 3 and 5 are utilized.

Fig. 10 shows the results that simulated the operation modes of the VCPSO and SPSO trackers of PV system under changing the solar irradiance of the solar panels under the PSC. Furthermore, the selected parameters of the DC-DC converter defined in section 4 is used in the proposed model under study. As can be seen from Fig. 10, the change in solar

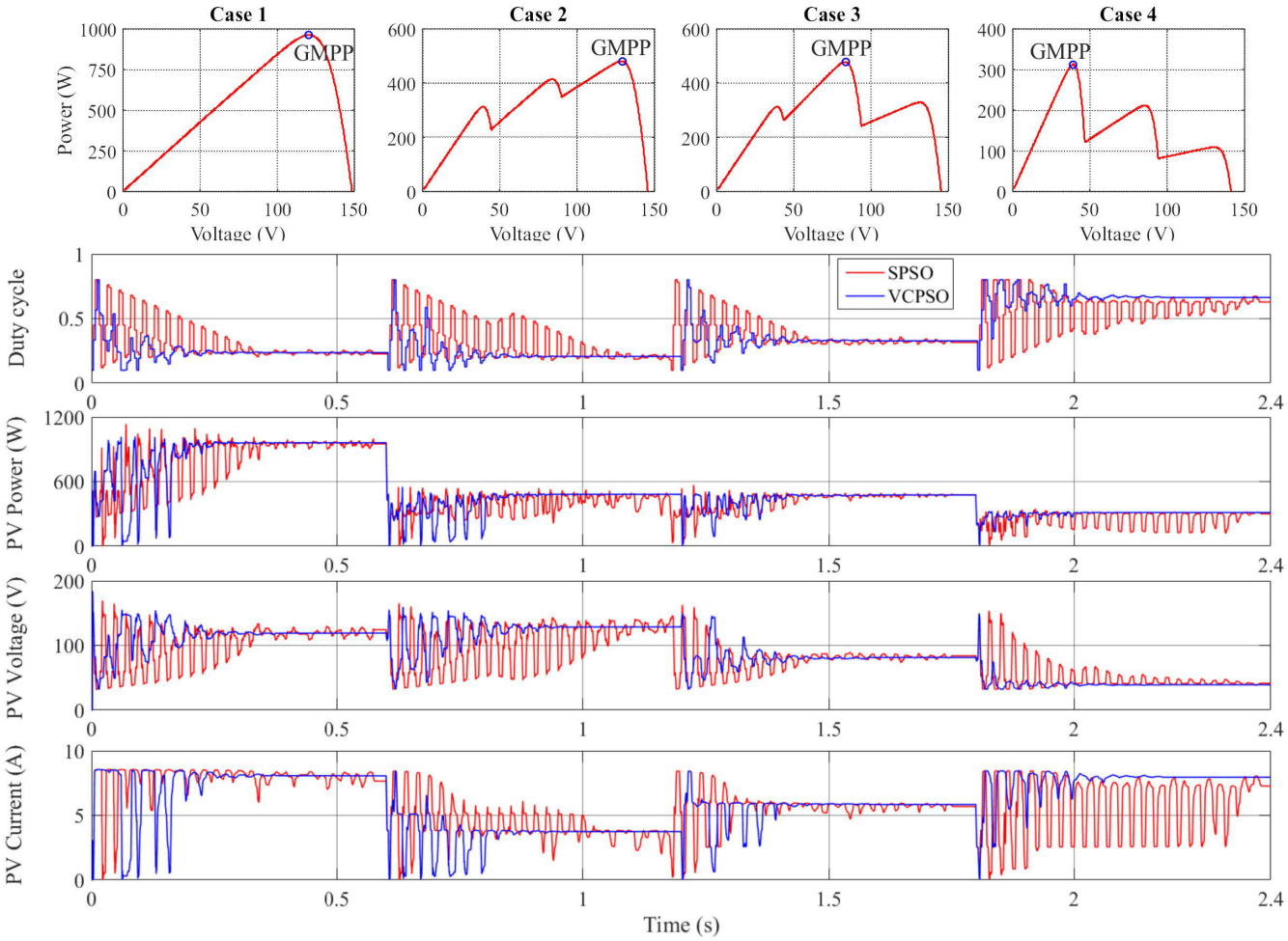

FIGURE 10. Detailed simulation results for PV system under the fast variation of the solar irradiance of the PV array.

irradiance is achieved each 0.6s for the first four cases of the PV1 configuration.

As it can be seen from Fig. 10, one can see that the VCPSO based tracker with the chosen parameter values provides a reliable and effective tracking of the GMPP for all four cases of studies compared to SPSO controller: the tracking efficiency of the VCPSO is higher than 99.5%, and the time track does not exceed 0.26s.

Based on the simulation results, one can see that the tracking time of the GMPP has been decreased when using the selected parameters in the VCPSO controller. To check the possibility of using a VCPSO algorithm with the given parameters in the MPPT controller of a PV system based on PV2 and PV3 configurations, the operating modes of the PV system with the last six studied cases 5-7 and 8-10, respectively have been simulated. In all proposed tests, the VCPSO controller ignores the local peak and catch the GMPP correctly. Furthermore, the average tracking efficiency of the controller was 99.85 % and the search time is not more than 0.28s. According to the simulation results, one can claim that the change in the duty cycle of the DC-DC buck converter is in a good agreement with the defined values of Section IV. While the duty cycle depends on the solar irradiance conditions, the fast track performance has been achieved as shown in the figure. These results indicate that the proposed methods of designing the PV system in this work are effective and accurate.

VII. CONCLUSION

The paper presents an original methodology for selecting the parameters of the main components of an autonomous PV system with an MPPT controller, which ensures the most efficient use of the available solar energy. The proposed PV system comprises PV array, MPPT controller, and buck converter connected to a battery bank that is implemented in Matlab/Simulink environment. A new method for selecting the parameters of a buck DC-DC converter connected to the battery bank is proposed. The nominal value of the voltage of the battery and the parameters of the converter is selected based on the calculation and analysis of the possible range of voltage variation of the MPP under various solar irradiance conditions and temperature. In this paper, two modified

versions of the PSO are presented to extract the GMPP of the PV array under the PSC. For these algorithms, the optimal sampling time, the optimal parameters, the optimal number of particles, and the number of iterations were evaluated. The selected optimal sampling time, i.e., 4ms, and the chosen four number of particles, for each controller helped in reducing the tracking time to extract the GMPP under the PSC. The results confirm that VCPSO based tacker provides high tracking efficiency in catching the GMPP in all studied cases compared with CFPSO based tracker. Finally; it is concluded that the improved VCPSO provides good prospects to implement this tracker in the MPPT control unit of the stand-alone PV system. The possible directions for future work would be (i) the implementation of the dynamic VCPSO -based tracker in practical applications; (ii) the application of other dynamic optimization techniques for tracking the global MPP; (iii) the employment of the dynamic optimization techniques in other applications such as control systems and power electronics.

ACKNOWLEDGMENT

The development of the control systems was carried out at Tomsk Polytechnic University within the framework of Tomsk Polytechnic University Competitiveness Enhancement Program. Also, the authors gratefully thank the reviewers for their time reviewing the article and the comments which help in improving the quality of their paper.

REFERENCES

[1] *Renewables 2018 Global Status Report*, REN21, Paris, France, 2018.
[2] A. Jäger-Waldau, "European commission, and joint research centre," Eur. Commission, Joint Res. Centre, Ispra, Italy, Tech. Rep. 2017, 2017.
[3] M. M. Shebani, T. Iqbal, and J. E. Quaicoe, "Comparing bisection numerical algorithm with fractional short circuit current and open circuit voltage methods for MPPT photovoltaic systems," in *Proc. IEEE Electr. Power Energy Conf. (EPEC)*, Oct. 2016, pp. 1–5.
[4] A. Loukriz, M. Haddadi, and S. Messalti, "Simulation and experimental design of a new advanced variable step size Incremental Conductance MPPT algorithm for PV systems," *ISA Trans.*, vol. 62, pp. 30–38, May 2016.
[5] T. H. Kwan and X. Wu, "High performance P&O based lock-on mechanism MPPT algorithm with smooth tracking," *Sol. Energy*, vol. 155, pp. 816–828, Oct. 2017.
[6] N. A. Kamarzaman and C. W. Tan, "A comprehensive review of maximum power point tracking algorithms for photovoltaic systems," *Renew. Sustain. Energy Rev.*, vol. 37, pp. 585–598, Sep. 2014.
[7] S. G. Obukhov, I. A. Plotnikov, and S. K. Sheryazov, "Methods of effective use of solar power system," in *Proc. 2nd Int. Conf. Ind. Eng., Appl. Manuf. (ICIEAM)*, 2016, pp. 1–6.
[8] M. A. Husain, A. Tariq, S. Hameed, M. S. B. Arif, and A. Jain, "Comparative assessment of maximum power point tracking procedures for photovoltaic systems," *Green Energy Environ.*, vol. 2, no. 1, pp. 5–17, Jan. 2017.
[9] M. Seyedmahmoudian, B. Horan, T. K. Soon, R. Rahmani, A. M. T. Oo, S. Mekhilef, and A. Stojcevski, "State of the art artificial intelligence-based MPPT techniques for mitigating partial shading effects on PV systems—A review," *Renew. Sustain. Energy Rev.*, vol. 64, pp. 435–455, Oct. 2016.
[10] F. Belhachat and C. Larbes, "Comprehensive review on global maximum power point tracking techniques for PV systems subjected to partial shading conditions," *Solar Energy*, vol. 183, pp. 476–500, May 2019.
[11] J.-Y. Shi, F. Xue, Z.-J. Qin, W. Zhang, L.-T. Ling, and T. Yang, "Improved global maximum power point tracking for photovoltaic system via cuckoo search under partial shaded conditions," *J. Power Electron.*, vol. 16, no. 1, pp. 287–296, Jan. 2016.
[12] Y.-P. Huang, X. Chen, and C.-E. Ye, "A hybrid maximum power point tracking approach for photovoltaic systems under partial shading conditions using a modified genetic algorithm and the firefly algorithm," *Int. J. Photoenergy*, vol. 2018, pp. 1–13, 2018.
[13] H. M. El-Helw, A. Magdy, and M. I. Marei, "A hybrid maximum power point tracking technique for partially shaded photovoltaic arrays," *IEEE Access*, vol. 5, pp. 11900–11908, 2017.
[14] W. Na, P. Chen, and J. Kim, "An improvement of a fuzzy logic-controlled maximum power point tracking algorithm for photovoltic applications," *Appl. Sci.*, vol. 7, no. 4, p. 326, Mar. 2017.
[15] N. Karami, N. Moubayed, and R. Outbib, "General review and classification of different MPPT techniques," *Renew. Sustain. Energy Rev.*, vol. 68, pp. 1–18, Feb. 2017.
[16] A. Ibrahim, R. Aboelsaud, and S. Obukhov, "Improved particle swarm optimization for global maximum power point tracking of partially shaded PV array," *Electr. Eng*, vol. 101, no. 2, pp. 443–455, Jun. 2019.
[17] G. Dileep and S. Singh, "An improved particle swarm optimization based maximum power point tracking algorithm for PV system operating under partial shading conditions," *Solar Energy*, vol. 158, pp. 1006–1015, Dec. 2017.
[18] M. Sarvi, S. Ahmadi, and S. Abdi, "A PSO-based maximum power point tracking for photovoltaic systems under environmental and partially shaded conditions," *Prog. Photovolt, Res. Appl.*, vol. 23, no. 2, pp. 201–214, Feb. 2015.
[19] H. Rezk, A. Fathy, and A. Y. Abdelaziz, "A comparison of different global MPPT techniques based on meta-heuristic algorithms for photovoltaic system subjected to partial shading conditions," *Renew. Sustain. Energy Rev.*, vol. 74, pp. 377–386, Jul. 2017.
[20] D. C. Huynh, T. M. Nguyen, M. W. Dunnigan, and M. A. Mueller, "Global MPPT of solar PV modules using a dynamic PSO algorithm under partial shading conditions," in *Proc. IEEE Conf. Clean Energy Technol. (CEAT)*, Nov. 2013, pp. 134–139.
[21] Y.-H. Liu, S.-C. Huang, J.-W. Huang, and W.-C. Liang, "A particle swarm optimization-based maximum power point tracking algorithm for PV systems operating under partially shaded conditions," *IEEE Trans. Energy Convers.*, vol. 27, no. 4, pp. 1027–1035, Dec. 2012.
[22] H. Chaieb and A. Sakly, "A novel MPPT method for photovoltaic application under partial shaded conditions," *Solar Energy*, vol. 159, pp. 291–299, Jan. 2018.
[23] K. Sundareswaran, V. Vignesh Kumar, and S. Palani, "Application of a combined particle swarm optimization and perturb and observe method for MPPT in PV systems under partial shading conditions," *Renew. Energy*, vol. 75, pp. 308–317, Mar. 2015.
[24] K. Ishaque, Z. Salam, M. Amjad, and S. Mekhilef, "An improved particle swarm optimization (PSO)–based MPPT for PV with reduced steady-state oscillation," *IEEE Trans. Power Electron.*, vol. 27, no. 8, pp. 3627–3638, Aug. 2012.
[25] S. M. Mirhassani, S. Z. M. Golroodbari, S. M. M. Golroodbari, and S. Mekhilef, "An improved particle swarm optimization based maximum power point tracking strategy with variable sampling time," *Int. J. Electr. Power Energy Syst.*, vol. 64, pp. 761–770, Jan. 2015.
[26] M. Abdulkadir, A. H. M. Yatim, and S. T. Yusuf, "An improved PSO-based MPPT control strategy for photovoltaic systems," *Int. J. Photoenergy*, vol. 2014, pp. 1–11, 2014.
[27] M. Mao, L. Zhang, Q. Duan, O. Oghorada, P. Duan, and B. Hu, "A two-stage particle swarm optimization algorithm for MPPT of partially shaded PV arrays," *Int. J. Green Energy*, vol. 14, no. 8, pp. 694–702, Jun. 2017.
[28] T. Sudhakar Babu, N. Rajasekar, and K. Sangeetha, "Modified particle swarm optimization technique based maximum power point tracking for uniform and under partial shading condition," *Appl. Soft Comput.*, vol. 34, pp. 613–624, Sep. 2015.
[29] A. Tobón, J. Peláez-Restrepo, J. Villegas-Ceballos, S. Serna-Garcés, J. Herrera, and A. Ibeas, "Maximum power point tracking of photovoltaic panels by using improved pattern search methods," *Energies*, vol. 10, no. 9, p. 1316, Sep. 2017.
[30] S. Obukhov, I. Plotnikov, and M. Kryuchkova, "Simulation of electrical characteristics of a solar panel," in *Proc. IOP Conf. Ser., Mater. Sci. Eng.*, vol. 132, Jun. 2016, Art. no. 012017.
[31] S. G. Obukhov and I. A. Plotnikov, "Simulation model of operation of autonomous photovoltaic plant under actual operating conditions," *Bull. Tomsk Polytech. Univ., Geo Assets Eng.*, vol. 328, no. 6, pp. 38–51, 2017.
[32] O. Tremblay, L.-A. Dessaint, and A.-I. Dekkiche, "A generic battery model for the dynamic simulation of hybrid electric vehicles," in *Proc. IEEE Vehicle Power Propuls. Conf.*, Sep. 2007, pp. 284–289.

[33] O. Tremblay and L.-A. Dessaint, "Experimental validation of a battery dynamic model for EV applications," *World Electr. Veh. J.*, vol. 3, no. 2, pp. 289–298, May 2018.
[34] J. Kennedy and R. Eberhart, "Particle swarm optimization," in *Proc. IEEE Int. Conf. Neural Netw.*, 1995.
[35] Y. Shi and R. Eberhart, "A modified particle swarm optimizer," in *Proc. IEEE Int. Conf. Evol. Comput. Proceedings. IEEE World Congr. Comput. Intell.*, Nov. 2002.
[36] G. Ahmad, "Photovoltaic-powered rural zone family house in Egypt," *Renew. Energy*, vol. 26, no. 3, pp. 379–390, Jul. 2002.
[37] A. Ghafoor and A. Munir, "Design and economics analysis of an off-grid PV system for household electrification," *Renew. Sustain. Energy Rev.*, vol. 42, pp. 496–502, Feb. 2015.
[38] S. Kolsi, H. Samet, and M. B. Amar, "Design analysis of DC-DC converters connected to a photovoltaic generator and controlled by MPPT for optimal energy transfer throughout a clear day," *J. Power Energy Eng.*, vol. 2, no. 1, pp. 27–34, 2014.
[39] R. Ayop and C. W. Tan, "Design of boost converter based on maximum power point resistance for photovoltaic applications," *Solar Energy*, vol. 160, pp. 322–335, Jan. 2018.
[40] M. Clerc and J. Kennedy, "The particle swarm—Explosion, stability, and convergence in a multidimensional complex space," *IEEE Trans. Evol. Comput.*, vol. 6, no. 1, pp. 58–73, Feb. 2002.
[41] G. Shankar and V. Mukherjee, "MPP detection of a partially shaded PV array by continuous GA and hybrid PSO," *Ain Shams Eng. J.*, vol. 6, no. 2, pp. 471–479, Jun. 2015.
[42] K. Ishaque and Z. Salam, "A deterministic particle swarm optimization maximum power point tracker for photovoltaic system under partial shading condition," *IEEE Trans. Ind. Electron.*, to be published.

SERGEY OBUKHOV was born in Tomsk, Russia, in 1963. He received the Ph.D. degree from National Research Tomsk Polytechnic University, Tomsk, in 1989. He continued his career at the department as a Senior Researcher. He is currently a Professor with National Research Tomsk Polytechnic University. He has 100 scientific publications in electric power engineering and electrical engineering. His research interest includes different types of renewable energy.

AHMED IBRAHIM was born in EL-Sharkia, Egypt, in 1987. He received the B.Sc. and M.Sc. degrees from the Faculty of Engineering, Zagazig University, Egypt, in 2009 and 2013, respectively.

He is currently a Teaching Assistant with National Research Tomsk Polytechnic University, Tomsk, Russia. He is working in the fields of optimization techniques, control systems, electric power grids, and renewable energy systems. He has more than 22 research articles and papers that are published in high-impacted journals and conferences.

AHMED A. ZAKI DIAB received the B.Sc. and M.Sc. degrees in electrical engineering from Minia University, Egypt, in 2006 and 2009, respectively, and the Ph.D. degree from the Electric Drives and Industry Automation Department, Faculty of Mechatronics and Automation, Novosibirsk State Technical University, Novosibirsk, Russia, in 2015. He had a postdoctoral fellowship at the Moscow Power Engineering Institute, National Research University (MPEI), Moscow, Russia, from September 2017 to March 2018. Since 2007, he has been with the Department of Electrical Engineering, Faculty of Engineering, Minia University, Egypt, as a Teaching Assistant and a Lecturer Assistant, and since 2015, as an Assistant Professor. He is currently a Visitor Researcher (Postdoctoral) with the Green Power Electronics Circuits Laboratory, Kyushu University, Japan (awarded the MIF Research Fellowship 2019, Japan). He is certified as a Siemens Engineer and a Trainer in several fields of automation and process control systems. He is the Supervisor of the Automatic Control and Traction Laboratory, Faculty of Engineering, Minia University. His current research interests include renewable energy systems, power electronics, and machines drives.

AMEENA SAAD AL-SUMAITI received the B.Sc. degree in electrical engineering from United Arab Emirates University, UAE, in 2008, and the M.A.Sc. and Ph.D. degrees in electrical and computer engineering from the University of Waterloo, Canada, in 2010 and 2015, respectively. She was a Visiting Assistant Professor with MIT, Cambridge, MA, USA, in 2017. She is currently an Assistant Professor with the Department of Electrical and Computer Engineering, Khalifa University, Abu Dhabi, UAE. Her research interest includes intelligent systems, energy economics, and energy policy. She was a recipient of the International Association of Geomagnetism and Aeronomy Young Scientist Award for Excellence, in 2008, and the IEEE Electromagnetic Compatibility Society Best Symposium Paper Award, in 2011.

RAEF ABOELSAUD was born in Zagazig, Egypt, in 1987. He received the B.Sc. degree (Hons.) and the M.Sc. degree in electrical engineering from Zagazig University, Zagazig, in 2009 and 2013, respectively. He is currently a Teaching Assistant with National Research Tomsk Polytechnic University, Tomsk, Russia. His current research interest includes power electronic converters and control systems applied to renewable energy conversion and energy storage.